Polymer Bulletin
https://doi.org/10.1007/s00289-023-04749-x

ORIGINAL PAPER

Determination of the crosslink density of silica-filled styrene butadiene rubber compounds by different analytical methods

Pilar Bernal-Ortega[1] · Rafal Anyszka[1] · Yoshihiro Morishita[2] · Raffaele di Ronza[2] · Anke Blume[1]

Received: 31 March 2022 / Revised: 24 January 2023 / Accepted: 28 February 2023

Abstract

The crosslink density of rubber compounds has a great effect on the properties of the final product. For this reason, a suitable characterization method is required to understand and optimize the final performance of rubber materials. Four different experimental techniques were used to determine the crosslink density of silica-filled styrene butadiene rubber composites: equilibrium swelling experiments, stress–strain measurements using the Mooney–Rivlin theory, freezing point depression temperature tests and Temperature Scanning Stress Relaxation (TSSR) measurements. The evaluation of these different techniques shows that the results obtained follow a similar trend for all four methods. The results from the Mooney-Rivlin and TSSR measurements correlate the best. These two techniques are the least affected by the presence of fillers and are the less time-consuming ones. Furthermore, they also show the best correlation with the mechanical properties of the studied compounds.

✉ Anke Blume
a.blume@utwente.nl

Pilar Bernal-Ortega
m.d.p.bernalortega@utwente.nl

Rafal Anyszka
r.p.anyszka@utwente.nl

Yoshihiro Morishita
yoshihiro.morishita@bridgestone.com

Raffaele di Ronza
Raffaele.DIRONZA@bridgestone.eu

[1] Department of Mechanics of Solids, Surfaces & Systems (MS3), Chair of Elastomer Technology and Engineering, Faculty of Engineering Technology, University of Twente, 7500 AE Enschede, The Netherlands

[2] Italian Branch–Technical Center, Bridgestone EU NV/SA, Via del Fosso del Salceto, 00128 Rome, Italy

Published online: 13 March 2023

Keywords Rubber · Silica · Silanes · Crosslink density

Introduction

Rubber is characterized by its high elasticity, being capable of recover its original shape after being stretched [1–3]. This elasticity of rubber is a unique phenomenon to which many researchers have tried to find an explanation. Many models and theories have been developed in the elastomer field in order to understand the behavior of the elastomeric networks [4–8]. This unique elasticity of rubber is obtained after a curing process. In this process, a three-dimensional network of crosslinks is created by loosely connecting the polymeric chains. The crosslink density mainly influences the final performance of rubber products, being a key property of rubber compounds [9, 10]. There are different methods to obtain and study crosslink density. Each method has its advantages and disadvantages such as lower or higher costs or longer or shorter measurement times. However, it is important to evaluate which methods are the most reliable ones and which show the best correlation with in-rubber properties. For this reason, a detailed study and understanding of the different techniques to measure crosslink density (CLD) is of great importance.

The crosslink density (ν) is defined as the number of crosslinks per unit of volume of rubber. It is usually expressed in (number of crosslinks)/(cm^3) of rubber. This parameter can be expressed also as the average molecular weight between cross-linking points (M_c). These two parameters are inversely proportional:

$$\nu \propto \frac{\rho}{M_c} \tag{1}$$

where ρ is the rubber density.

Depending on their structure, crosslinks can be classified into carbon–carbon or sulfidic crosslinks. In the case of sulfidic crosslinks, they are classified as monosulfidic (C–S–C), disulfidic (C–S_2–C) and polysulfidic (C–S_x–C, $x \geq 3$). The type of crosslink also has a great influence on the final properties of the material [11].

There are different techniques and methodologies to quantify and analyze the crosslink density of rubber compounds. The most common techniques used for the determination of this parameter are equilibrium swelling experiments based on the Flory–Rehner model [12] and stress–strain tests using the Mooney–Rivlin approach [13, 14]. However, the last few years have brought up some novel techniques such as dielectric measurements [15], low field NMR [16], differential scanning calorimetry [17–19] or temperature scanning stress relaxation (TSSR) [20–23].

The aim of this work is the comparison of different experimental techniques to determine the crosslink density of rubber compounds with the purpose to identify which method correlates in the best way with in-rubber properties. For this reason, four different techniques to obtain CLD were studied and compared, analyzing the obtained results and also their advantages and disadvantages such as price or time of the experiment. The following four approaches were chosen: equilibrium swelling experiments, stress–strain tests based on the Mooney–Rivlin approach, freezing point depression

temperature method and temperature scanning stress relaxation measurements. In order to analyze the effect of different silanization processes on the rubber network, different compounds were prepared using in-situ and ex-situ silanization of the silica. These compounds were compared to an unmodified silica-filled compound. In general, the crosslink density of silica-filled compounds is affected by several factors: the filler–filler network, the polymer–polymer network and silica/silane/polymer coupling.

Equilibrium swelling

Equilibrium swelling experiments are the most widely used technique to obtain crosslink density in the rubber field due to their simplicity and low cost. However, these experiments are quite time consuming. The normal duration of equilibrium swelling measurements contains a minimum of 7 days. These measurements are built on the characteristic increase in the volume of the rubber network when a crosslinked rubber is immersed in a suitable solvent. The solvent molecules penetrate between the connected polymer chains causing the intensive expansion of the rubber network. The determination of the CLD by swelling experiments is usually based on the Flory–Rehner model for swollen polymer networks [24, 25].

Mooney–Rivlin

Stress–strain measurements are one of the most common methods to study the crosslink density of rubber compounds together with equilibrium swelling experiments. The different approaches to determine crosslink density by mechanical tests are based on the theory of rubber elasticity [8].

The Mooney–Rivlin theory was developed by J. Mooney and R.S Rivlin to describe the rubber network of unfilled compounds by the presence of crosslinks and entanglements [13, 14]. They proposed a semi-empirical equation (Eq. 2) that allows the determination of the crosslink and entanglements density:

$$\frac{F}{2A_0(\lambda - \lambda^{-2})} = \frac{1}{\lambda}C_2 + C_1 \tag{2}$$

where F is the force, A_0 is the cross-sectional area of the sample, λ is the extension ratio, R is the ideal gas constant, T is the temperature, and C_1 and C_2 are the elastic constants. The constants C_1 and C_2 correlate with the crosslink and entanglements density according to the next equations:

$$\nu_c = \frac{2C_1}{\mathrm{RT}} \tag{3}$$

$$\nu_e = \frac{2C_2}{\mathrm{RT}} \tag{4}$$

where ν_c and ν_e are the crosslinks and entanglements density.

As previously discussed, this theory was developed for unfilled rubbers. The introduction of filler particles changes the elastic behavior of rubber compounds. For this reason, a specific pre-treatment is required for filled rubber samples. The samples undergo several (usually 9) cycles before the final measurement takes place. The main goal of these cycles is the destruction of the filler network. By achieving this, only the effects of the polymer network remain [22]. Furthermore, the addition of particles leads to an enhancement of the modulus compared to unfilled compounds. This enhancement depends on the filler volume fraction added. This phenomenon is known as the hydrodynamic modulus amplification [26, 27]. The increase in the modulus is also associated with an improvement of the deformation of the polymer chains around the (non-deformable) filler particles, known as strain amplification [27]. For these reasons, in filled compounds, the extension ratio λ should be replaced by λ^*, taking into account the strain amplification ratio (Eq. 5) [27]:

$$\lambda^* = \varepsilon x + 1 \tag{5}$$

where ε is the relative strain and, x is the strain amplification factor that can be calculated by the use of the Guth and Gold equation for spherical particles:

$$x = 1 + 2.5\phi_f + 14.1\phi_f^2 \tag{6}$$

where ϕ_f is the filler volume fraction.

Freezing point depression temperature

The freezing point depression of solvents imbibed in swollen vulcanizates has been studied by many authors [17, 19, 28–30]. These studies show that the magnitude of depression of the solvent's freezing point in a swollen vulcanizate is related to the degree of crosslink density. By comparing the transition temperature values of a confined and free solvent, the freezing point depression temperature (ΔT_f) can be calculated. This is the difference between the freezing temperature of the pure solvent and that of the solvent that is trapped in the rubber compound. This parameter depends on the mesh size of the polymer network. When the polymer chains are connected to each other by a higher number of crosslinks, the mesh size becomes smaller, and the solvent is confined in a tighter network constraining the crystallization of the solvent [29]. The network chains mechanically restrict the formation of the crystals and as a consequence their size. The formation of smaller crystals leads to a higher vapor pressure and, as a result, to a decrease in the freezing temperature [30–32]. The freezing point of the solvent is the sum of the freezing point of the "free" solvent and that of the "trapped" solvent. If less solvent is trapped, this freezing temperature becomes lower which means that the freezing point depression is larger and the crosslink density is higher. However, the intensity of the peak corresponding to the freezing temperature of the trapped solvent decreases. The higher the crosslink density, the smaller the mesh size, and therefore, less amount of solvent is trapped in the network [33]. This behavior is illustrated in Fig. 1, where the DSC curve of pure cyclohexane is compared to two swollen rubber samples, with

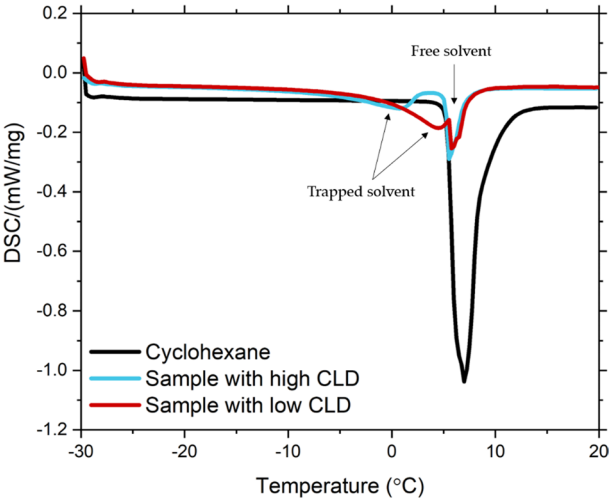

Fig. 1 DSC freezing curve for pure cyclohexane (black line), rubber sample with high CLD (blue line) and rubber sample with low CLD (red line) (Colour figure online)

high and low CLD. As can be observed, the curve for the pure cyclohexane (black line) contains only one peak, corresponding directly to its freezing temperature. However, when analyzing the curves for the swollen rubber, two differentiate peaks can be observed: the peak of the free solvent and the peak of the solvent trapped in the rubber network. For the sample with the higher CLD (blue line), the peak of the trapped solvent appears at lower temperature and the intensity is lower compared to the sample with low CLD (red line).

Temperature scanning stress relaxation (TSSR)

Temperature Scanning Stress Relaxation is a newly developed method for the characterization of polymeric materials. The calculation of the CLD using TSSR experiments is based on the evaluation of the stress relaxation of rubber when a constant strain and an increasing temperature are applied [21, 23, 34].

Elastomers show a stress relaxation when a constant strain is applied, observing a decrease in the stress with increasing time caused by physical and/or chemical processes [22, 23, 34]. Usually, these kinds of experiments are evaluated at constant temperature. However, the last few years an alternative measurement procedure have been developed [20, 23, 34]. These TSSR measurements are based on the non-isothermal relaxation behavior of rubber compounds. When a crosslinked rubber is exposed to a constant strain with increasing temperature, it contracts. This behavior is characteristic for rubber compounds and is known as the Gough–Joule effect [35]. For stresses higher than 10% ($\varepsilon > 10\%$), a thermoelastic inversion occurs: the entangled structures and chain segments of the network relax which reduces the entropy of the system. With rising temperature, the mobility of the molecules increases which try to recover to its original entropical state causing a contraction of

the rubber. This phenomenon provokes that at a constant strain and rising temperature, an increase in the stress is observed. According to the theory of rubber elasticity for an ideal elastic network, the mechanical stress (σ) is proportional to the absolute temperature and the crosslink density of the network at constant strain [34, 36]:

$$\sigma = \nu \mathrm{RT}\left(\lambda - \frac{1}{\lambda^2}\right) \tag{7}$$

Where ν is the crosslink density, R is the ideal gas constant, T is the temperature, and λ is the strain ratio ($\lambda = l/l_0$). For the application of this method for filled compounds, the same corrections used in the Mooney–Rivlin theory regarding extension ratio λ were considered, following Eqs. 5 and 6.

Materials

Materials

The rubber used in this work was non-functionalized SSBR BUNA 3038-2 HM (Arlanxeo, Dormagen, Germany). The selected silica was ULTRASIL 7000 GR (Evonik Industries, Wesseling, Germany). Bis(triethoxysilylpropyl) disulfide (TESPD) (Evonik Industries, Antwerpen, Belgium) was used as silane coupling agent and hexadecyltrimethoxysilane (Millipore Sigma, Hamburg, Germany) as covering agent (CA). For the preparation of the rubber compounds, Zinc oxide (ZnO) and stearic acid were used as activators (both from Millipore Sigma, Hamburg, Germany); sulfur and N-tert-butyl-benzothiazole sulfonamide (TBBS) (both from Caldic B.V., Rotterdam, The Netherlands) as curatives and treated distillate aromatic extracted oil (TDAE) (Hansen & Rosenthal, Hamburg, Germany).

Pre-silanization of silica

The modification process of the silica was the same for both modifying agents, TESPD and CA. The procedure was performed in one single step using toluene as the reaction medium. The silica and the modifying agent were mixed together with continuous stirring in toluene and then, heated up to 80 °C for 24 h. Afterward, the sample was filtered and dried in an oven to eliminate all the solvent.

Compounding and mixing

Rubber compounds were prepared in an internal mixer (Brabender Plasti-Corder 350S, Duisburg, Germany) with a fill factor of 0.7, an initial temperature of 100 °C and a rotor speed of 50 rpm. For the present study, the following samples were prepared, according to the formulation shown in Table 1 and the mixing procedure in Table 2:

- R1: filled with unmodified silica and without silane

Table 1 Formulation of the studied compounds in phr

Compounds	SBR (phr)	Silica* (phr)	TESPD* (phr)	Covering agent* (phr)	TDAE (phr)	Other ingredients (phr)
R1	100	80	–	–	37.5	Zinc Oxide-2.5 Stearic Acid-2.5 Sulfur-1.4 TBBS-2
R2	100	80	6.2	–	37.5	
R3	100	80	–	2	37.5	
R4	100	87.2	–	–	37.5	
R5	100	89.5	–	–	37.5	
R6	100	87.2	2	–	37.5	
R7	100	87.2	–	2	37.5	
R8	100	89.5	–	2	37.5	

*In the samples R4, R5, R6, R7 and R8, TESPD or the covering agent was already bonded to the silica. The quantity of the modifying agent bonded to the silica was determined by thermogravimetric analysis (TGA)

Table 2 Mixing procedure of the rubber compounds

Time (min)	Action
Step 1 pre-heating 100 °C–50 rpm	
0.00	Addition of rubber, mastication
1.20	Addition of 1/3 filler, 1/2 silane (TESPD or covering agent)
2.40	Addition of 1/3 filler, 1/2 silane, (TESPD or covering agent), TDAE
4.00	Addition of 1/3 filler, Zinc Oxide, Stearic Acid
5.00	Increase in the torque (increase temperature to 130 °C)
10.00	Stop mixing (reaching 140 °C)
Step 2 pre-heating 50 °C–50 rpm	
0.00	Addition of elastomer pre-mix, mastication
1.30	Addition of curatives (sulfur, TBBS)
3.00	Stop mixing

- R2: in situ silanized during mixing with TESPD
- R3: filled with unmodified silica and addition of covering agent during mixing
- R4: pre-silanized silica with TESPD
- R5: pre-silanized silica with covering agent
- R6: pre-silanized silica with TESPD + addition of TESPD during mixing
- R7: pre-silanized silica with TESPD + addition of covering agent during mixing.
- R8: pre-silanized silica with covering agent + addition of covering agent during mixing

Methods

Equilibrium swelling experiments

The crosslink density by equilibrium swelling experiments was obtained using the Flory–Rehner equation (Eq. 8) [12]. The samples were previously extracted with acetone for 24 h. The extraction with acetone removes low molecular, non-rubber soluble substances, such as zinc salt of the accelerator and its decomposition products, zinc fatty acid soaps, antioxidants, polymerization aids and oils. [37]. Five vulcanized samples (~0.25 g) of each compound were swollen in 150 ml of toluene at room temperature for a period of 7 days, changing the solvent on a regular basis:

$$\nu = -\frac{\ln\left(1 - V_r\right) + V_r + \chi V_r^2}{V_0\left(V_r^{\frac{1}{3}} - \frac{2V_r}{f}\right)} \tag{8}$$

where ν is the crosslink density in mol/cm^3, V_r is the volume fraction of rubber in a swollen sample, V_0 is the solvent molar volume, f is the functionality of crosslinks ($f = 4$, assuming the formation of tetra functional crosslinks), and χ is the Flory–Huggins interaction parameter. In this work, χ was calculated by using Eq. 9 [38]:

$$\chi_{12} = \frac{[V\left(\delta_1 - \delta_2\right)^2]}{\mathrm{RT}} + 0.34 \tag{9}$$

where V is the molar volume of the solvent, δ_1 is the solubility parameter of the rubber, δ_2 is the solubility parameter of the solvent, R is the ideal gas constant, and T is the temperature.

The volume fraction of rubber, V_r, was calculated using Eq. 10:

$$V_r = \frac{1}{1 + Q_v} \tag{10}$$

where Q_v is the equilibrium volume swelling, obtained with Eq. 11:

$$Q_v = Q_w \frac{\rho_r}{\rho_s} \tag{11}$$

where Q_w is the equilibrium mass swelling, ρ_r is the density of the rubber, and ρ_s is the density of the solvent. The value of Q_w was determined using Eq. 12:

$$Q_w = \frac{m_s - m_d}{m_d - m_0 f} \tag{12}$$

where m_s is the mass of the sample in the swollen state, m_d is the mass of the dried sample after swelling, and m_0 is the mass of the original sample before swelling, and f is the fraction of insoluble particles (filler + ZnO).

Freezing point depression temperature

The determination of the freezing point depression temperature was carried out using a Differential Scanning Calorimetry DSC 214 Polyma, from Netzsch-Gerätebau (Selb, Germany). Small pieces of the vulcanized rubber (previously acetone-extracted), around 2 × 2 × 1.5 mm, were swollen in ~ 150 ml of cyclohexane for 3 days to reach the equilibrium swelling. The swollen samples were then placed into DSC pans with an excess of cyclohexane to ensure that the solvent is trapped inside the polymer network. Cyclohexane was used as solvent because it shows a clear crystallization peak in DSC, and it is a good swelling solvent for SBR [17, 29, 33, 39]. The samples were cooled until −30 °C; then, the temperature was maintained for 5 min and afterward increased until 20 °C. The cooling/heating rate was 5 °C/min under nitrogen atmosphere.

Mooney–Rivlin

The determination of the crosslink density by Mooney–Rivlin approach was carried out by stress–strain essays performed in a universal testing machine Zwick Z010 (Zwick, Germany). Test specimens were 2 mm thick, with a test length of 20 ± 0.5 mm and a width of the narrow portion of 4 ± 0.1 mm, according to the ISO 37 (dye type 2) standard. The stress–strain essays consisted in two different steps:

(i) In the first step, the samples were pre-cycled 10 times until 200% strain at a crosshead speed of 500 mm/min. This first step is performed in order to destroy the filler network.
(ii) In the second step, the specimens were stretched until a strain of 200% at a crosshead speed of 10 mm/min.

Temperature scanning stress relaxation (TSSR)

The crosslink density obtained by Temperature Scanning Stress Relaxation experiments was measured using a TSSR instrument from Brabender Messtechnik (Duisburg, Germany). Test specimens were 2 mm thick, with a test length of 20 ± 0.5 mm and a width of the narrow portion of 4 ± 0.1 mm, according to the ISO 37 (dye type 2) standard. The experiments were performed in two steps (Fig. 2):

(i) In the first step, the sample was placed in a heating chamber at room temperature (T_0 = 23 °C). A strain of 50% (ε = 50%) was applied for 2 h. In this first step, a short time relaxation process occurs reaching a quasi-equilibrium state for the sample.
(ii) The second step starts directly after the isothermal relaxation: The 50% strained sample was heated with a constant rate of 2 K/min until reaching 100 °C.

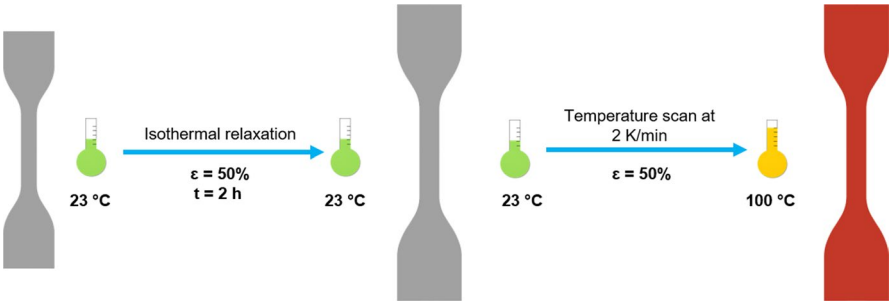

Fig. 2 Schematic representation of the TSSR procedure

The crosslink density was calculated using Eq. 8. For this, the finally reached value of the stress (σ) at 100 °C was taken. When rubber samples reach a certain temperature, the stress relaxation dominates their behavior, and the entropy effect can be neglected. At this point, the stress reaches a plateau and remains constant. The stress at this temperature is proportional to the crosslinks formed in the compounds [23].

Results

Pre-silanization of silica

The success of the functionalization process was analyzed by Fourier Transform Infrared Spectroscopy (FTIR) (PerkinElmer, Waltham, MA, USA) using the DRIFTS (diffuse reflectance infrared Fourier transform spectrometry) cell. The modification was confirmed for both samples by the presence of the band at a ~ 2965 cm^{-1}, corresponding to the symmetric and asymmetric stretching of $–CH_2$ groups and the band at ~ 1480 cm^{-1}, assigned to $–CH_3$ groups (Fig. 3a).

The quantification of the amount of silane attached to the silica was performed using Thermogravimetric Analysis (TGA) using a TA 550 device (TA Instruments, New Castle, DE, USA) operating under an air atmosphere with a heating rate of 20 °C/min from room temperature to 800 °C. The quantity of modifying agents at the surface of the silica was approximately 9% for the TESPD and 10% for the covering agent (Fig. 3b). These values were used as basis to add the correct amount of filler to the compounds, in order to have an isomolar content to the in-situ samples.

Crosslink density

Expected crosslink density

According to the different interactions present in each compound (silica–rubber and silica–silane coupling and filler–filler interactions), an estimation of which samples will have a higher or a lower crosslink density was done (Table 3).

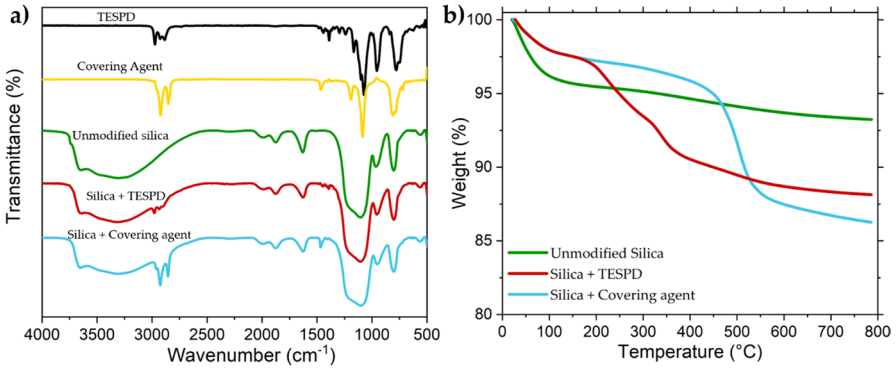

Fig. 3 **a** Fourier Transform Infrared Spectroscopy (FTIR) analysis of the of the unmodified (green line) and modified silicas with bis(triethoxysilylpropyl) disulfide (TESPD) (red line) and covering agent (blue line), TESPD (black line) and covering agent (CA) (yellow line) and **b** thermogravimetric analysis (TGA) curves of the unmodified (green line) and modified silicas with TEPSD (red line) and covering agent (blue line) (Colour figure online)

Table 3 Different interactions present in the studied rubber compounds

Sample	Silica–rubber coupling	Silica–silane coupling	Filler–filler interactions
R1	None	None	High
R2	Medium	Medium	Medium
R3	None	Low	High
R4	Medium	Medium	Medium
R5	None	High	Low
R6	High	High	Low
R7	High	High	Low
R8	None	High	Low

In the case of sample R1 (unmodified silica), it is expected to have the lowest crosslink density of all compounds. In this compound, there should not be any pronounced rubber-filler interactions present and the filler network should be extremely strong due to the absence of a bi-functional silane. Furthermore, due to the absence of a silane in this compound, accelerators can be absorbed by the silica surface leading to a lower CLD.

Regarding the samples in which TESPD is used as a coupling agent, two groups can be differentiated. In one group, the samples are R2 (in-situ silanized with TESPD) and R4 (pre-silanized with TESPD). These two compounds should show a similar CLD and a higher one than that of R1. The presence of TESPD should lead to the formation of covalent bonds between the silica and the rubber, which should increase the overall CLD. In the other group, R6 and R7 are the both pre-silanized with TESPD and with extra addition of TESPD (R6) or with extra addition of covering agent (R7) during mixing. In a previous study [33], it was analyzed that for pre-modified silica, new unmodified surface can be exposed during the mixing process

which might cause the formation of a more pronounced filler network. When additional silane is added to this freshly created silica surface, it can cover this surface and suppress the formation of stronger filler–filler interactions. For this reason, R6, it is expected to have the highest CLD of all the compounds. The addition of TESPD during the mixing process can cover the freshly created silica surface (reducing the filler network) and also couple to the polymer which should result in additional covalent bonds that can increase the CLD. In the case of R7, the CLD should be lower than R6 because the additional covering agent can reduce the filler network by covering the freshly created silica but cannot couple to the rubber due to its monofunctional nature. A further aspect has to be considered: The presence of additional TESPD and CA can shield the silica surface more effectively, hindering the absorption of accelerators and ZnO and leading to an increase in their active concentration in the compound. For this reason, a higher crosslink density could be obtained for these two compounds in comparison with R2 and R4.

Finally, for the compounds with covering agent in the formulation (R3, R5 and R8), a lower CLD compared to the samples with TESPD is expected, but a higher one than that of R1. The CLD in these compounds should be lower than the ones with TESPD because of the absence of a silica–rubber coupling due to the monofunctional nature of the covering agent. However, it is expected to be higher than R1, because in these samples, the silica surface is covered by the covering agent, and as explained above, this avoids the absorption of accelerators and ZnO.

Summarizing, the order of the expected CLD of the compounds from high to low is: R6 > R7 > R4 > R2 > R8 > R5 > R3 > R1.

Freezing point depression temperature (ΔT_f)

Figure 3 illustrates the theoretical behavior of a solvent imbibed in a swollen vulcanizate during freezing point depression experiments. On the one hand, a highly crosslinked polymer network (Fig. 4a) shows a smaller mesh size. As a consequence, the crystallization of the solvent is hindered and less solvent can be trapped in the rubber network. On the other hand, when a network contains a lower crosslink density (Fig. 4b), the mesh size is bigger and more solvent molecules can penetrate inside one individual mesh and therefore, in the whole network.

The DSC freezing curves and the freezing point depression of the swollen rubber compounds are shown in Fig. 5. In all DSC curves, two different peaks can be observed: The peak of the free solvent and the peak of the solvent trapped in the rubber network (Fig. 5a). The depression of the freezing temperature of the solvent is clearly visible for all samples.

The sample R1 (unmodified silica) shows a relatively high freezing depression point, just lower than the compounds containing TESPD in the formulation. The lower CLD compared to these compounds (R2, R6 and R7) is caused by the absence of a bi-functional silane in R1, and therefore the non-existence of a coupling between the silica and the rubber. The covalent bonds formed due to the presence of TESPD increase the crosslink density of these compounds (R2, R4, R6 and R7) leading to a smaller mesh size. As a consequence, the crystallization of the solvent is hindered and the freezing point depression is larger. Furthermore, it can be

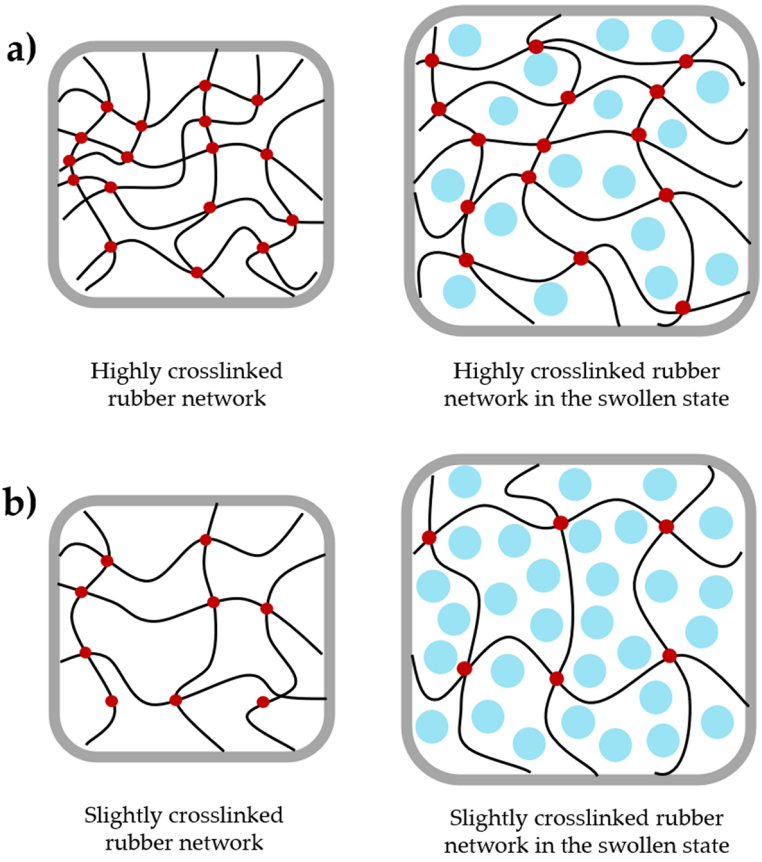

Fig. 4 Schematic representation of the freezing point depression analysis for the determination of CLD

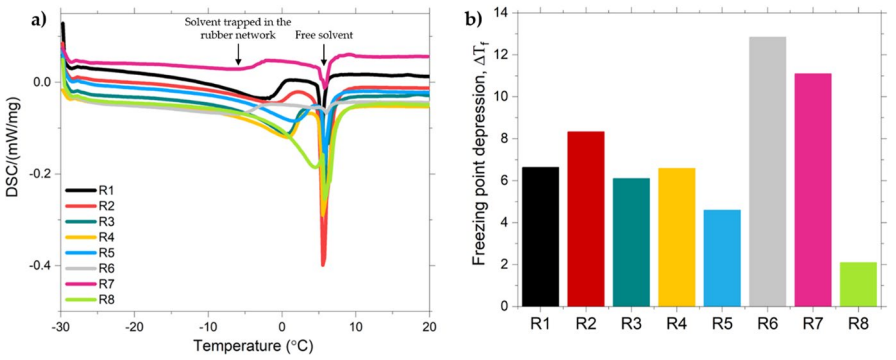

Fig. 5 **a** DSC freezing curves for the swollen compounds and **b** Freezing point depression of the compounds

noticed that the intensity of the peak of the trapped solvent in these samples is lower. As explained above, this is caused by the smaller amount of solvent trapped in the network. However, the CLD for the sample R1 is significantly higher than expected, reaching similar values than the ones obtained for sample R4 (pre-modified with TESPD). The high freezing point depression can be explained by the presence of a mechanical or physical three-dimensional mesh formed by the strong filler–filler interactions in R1 [39, 40]. This mesh restricts the swelling, leading to a higher freezing point depression which assumes a higher value of crosslink density for this compound. This behavior could also explain why R4 has a lower CLD than R2. The pre-modification of the silica with TESPD in R4 led to a more effective silanization of the silica surface and consequently to a decrease in the filler–filler interactions [33].

As expected, the samples that present the largest freezing point depression are R6 and R7, both pre-modified with TESPD and with the supplementary addition of TESPD (R6) or CA (R7) during mixing. As explained above, this result is caused by the extra addition of TESPD and CA during mixing in these compounds. This principle was followed in the sample R6: The addition of TESPD during the mixing process can cover the freshly created silica surface and couple to the polymer which results in additional covalent bonds, indicated by the highest crosslink density. For the compound R7, the addition of the covering agent during mixing covers the freshly created silica surface as well but does not couple to the rubber resulting in a lower CLD than R6.

Regarding the samples which contain covering agent (R3, R5 and R8), they present the lowest values of the freezing point depression. These results can be explained by the absence of a polymer–filler coupling and a weak filler network. The sample R8 presents an extremely low crosslink density. This result is explained by the additional covering agent added during the mixing process. As previously before, when additional covering agent is incorporated, it can cover the new freshly created silica surface reducing the interaction between particles in a higher degree [33]. In the case of R3, the small addition of CA during mixing is not sufficient to avoid filler–filler interactions. For this reason, it presents a higher CLD than R5 and R8.

Analyzing the obtained results for this method and comparing with the interactions present in each compound (Table 3), it can be concluded that the silica–rubber coupling is the interaction which has the highest impact on the CLD. This is observed in the results obtained for samples R6 and R7 that present the highest filler–rubber interactions and the highest values of CLD of all samples. However, it also can be noticed that these measurements are influenced by the filler network. This is observed in samples R1 and R3. These two samples show an extremely strong filler network and also an unexpected high CLD.

Equilibrium swelling experiments

The crosslink density of the studied compounds obtained by equilibrium swelling is shown in Fig. 6. As observed in the DSC results, the sample R1 shows a higher CLD than expected, just lower than the compounds with TESPD. However, in

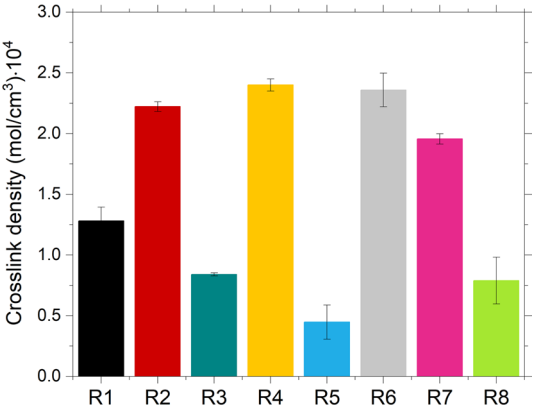

Fig. 6 Crosslink density measured by equilibrium swelling experiments

this method, the difference between R1 and R2 and R4 is much higher. This result could be caused by the filler effects on the equilibrium swelling experiments. Several investigations claimed that the presence of particles in the rubber compounds, that are non-swellable elements, can lead to a miscalculation of the crosslink density [39, 41–43]. The presence of fillers causes a restriction on the swelling behavior of rubber compounds leading to an overestimated calculated CLD. A schematic representation of this behavior is illustrated in Fig. 7. For this reason, R1 (with a strong filler network) presents a higher CLD than expected, but also R2 and R4. For compounds R2 and R4, the combination of a medium level of particle–particle interactions plus the presence of a polymer–filler coupling leads to a much higher CLD than R1. Moreover, these two samples show similar values than R6 and are superior to R7, which have an extra addition of coupling agent during mixing and therefore, lower filler–filler interactions. This behavior is especially evident in sample R7 that presents the lowest value of the compounds containing TESPD. This can be explained by the much better shielding effect of the long alkyl chain of the CA compared to the TESPD. As a result, the filler–filler interactions are reduced in a higher degree in this sample.

As already observed with the freezing point depression study, samples with covering agent (R3, R5 and R8) show the lowest CLD. Again, some differences are there. R8 shows a much higher crosslink density than R5. A possible explanation for this result could be that in sample R5, the accelerators may be absorbed by the new silica surface created during mixing causing a decrease in the CLD. In sample R8, this situation is avoided by the addition of covering agent during mixing.

Correlating the results obtained for equilibrium swelling and the interactions present in the samples (Table 3), it can be concluded that the filler–filler interactions dominate the results obtained by this swelling measurement. The samples in which these interactions are reduced (R5 and R8) have the lowest values of CLD. Furthermore, the filler effects also cause that samples R1, R2 and R4 show a higher CLD than expected. In this measurement, sample R2 and R4 reach a similar value of CLD than R6 and superior to the value obtained for sample R7.

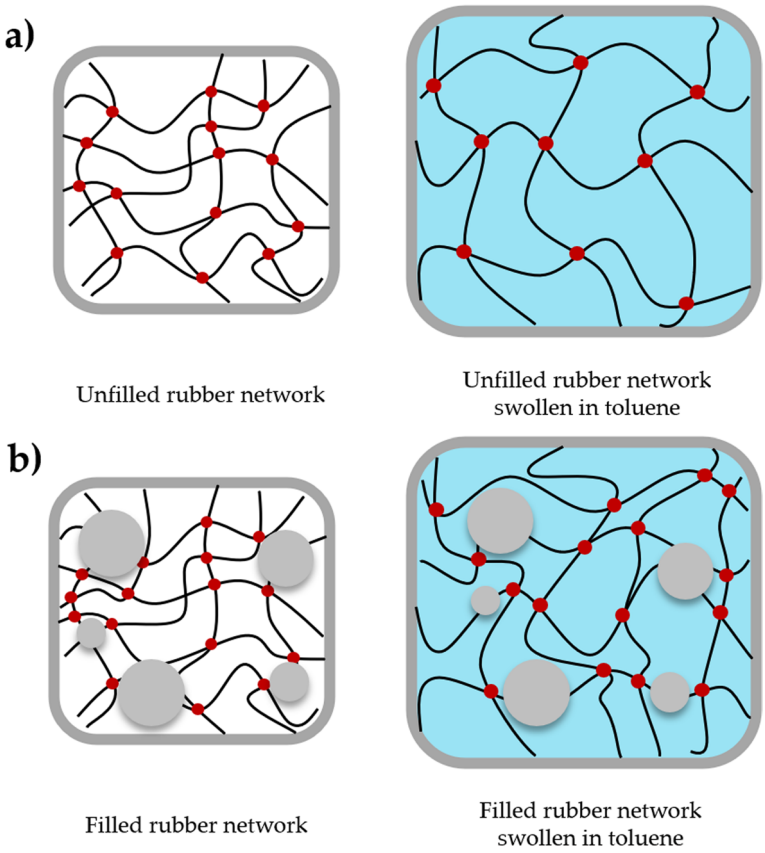

Fig. 7 Schematic representation of the equilibrium swelling analysis to obtain CLD for **a** unfilled and **b** filled rubber networks

Mooney–Rivlin

The results obtained by stress–strain experiments based on the Mooney–Rivlin theory are depicted in Fig. 8. As observed before for DSC and swelling experiments, sample R1 shows a much higher CLD than expected. However, this result is more similar to the one obtained in the freezing point depression. Sample R1 reaches CLD values similar to R4 and R7 and just lower than R2 and R6. As discussed already for the other analyzed techniques, this result could be explained by the strong filler–filler interactions due to the absence of a coupling agent in this sample. It might be that the cyclical stretching sequence performed to destroy the filler network before the measuring of the final polymer network took place was not sufficient in this compound or that there was a re-forming of the filler network caused by the long duration of the measurements. If this strong filler network might not be fully destroyed by the application of the stress–strain pre-cycles to the samples, it can be the cause of this high value of CLD obtained for R1.

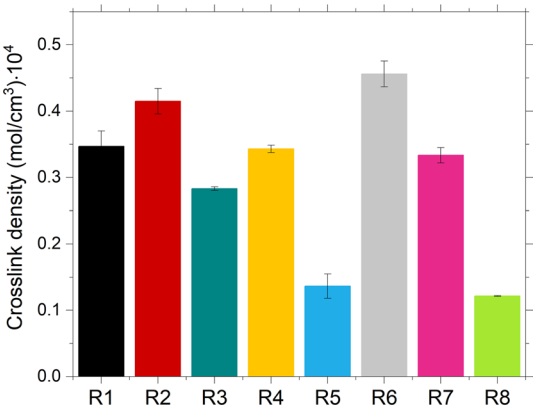

Fig. 8 Crosslink density measured by stress–strain experiments using the Moone-Rivlin approach

Regarding samples R2, R4, R6 and R7 (containing TESPD), they present the highest values of CLD due to the presence of covalent bonds between the silica and the rubber. Once again, sample R6 (pre-modified with TESPD + addition of TESPD during mixing) shows the highest CLD of all samples. As already explained, this is due to the new covalent bonds formed by the addition of extra TESPD during mixing. However, some differences with the other techniques can be noticed. In this Mooney–Rivlin method, the results of samples R4 and R7 are approximately the same. The main difference between these samples is that R7 has lower filler–filler interactions caused by the extra addition of CA during mixing. Therefore, a possible explanation is that the CLD calculated for R4 is overestimated due to the filler effects. For this reason, sample R4 with the same level of polymer–filler interactions but with a stronger filler network, reaches similar values than sample R7.

As for the samples with CA, they show the lowest crosslink density. Again, the Mooney–Rivlin results for these compounds are more similar to the ones obtained by the freezing point depression. Sample R3 shows a much higher CLD than R5 and R8, which have significantly less filler–filler interactions due to the larger content added of CA in these compounds.

As already observed for the freezing point depression and the equilibrium swelling experiments, the stress–strain experiments are also affected by the different interactions present in the compounds. The results obtained are mainly influenced by the filler–filler interactions and the presence or absence of a filler–polymer coupling. However, the filler effects seem to have here a lower impact than in the swelling experiments. In this method, the interactions that seem to dominate the obtained results are the silica–rubber bonds, as it is observed by the higher CLD obtained for sample R6 (Table 3).

Temperature scanning stress relaxation (TSSR)

The values of the crosslink density calculated using Eq. 8 with the data obtained from TSSR measurements are shown in Fig. 9. It is clearly revealed that the results of this technique present similarities with the ones obtained with the other three

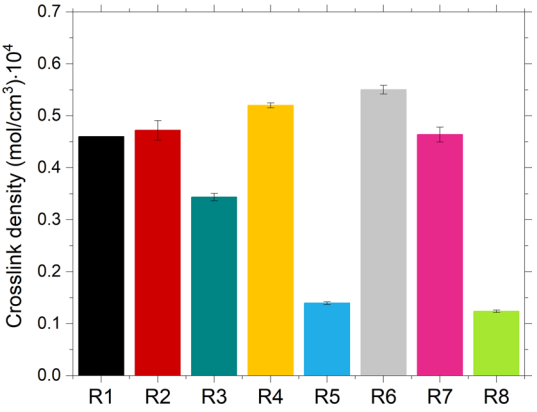

Fig. 9 Crosslink density measured by TSSR experiments

methods. Starting with sample R1 (unmodified silica), once more a higher value of CLD than expected is reached. With this technique, sample R1 presents almost the same crosslink density than sample R2 and R7 and lower than R4 and R6. As previously discussed, this behavior can be associated with the strong filler network being present in this compound that can lead to the assumption of a higher crosslink density.

Regarding the samples containing TESPD (R2, R4, R6 and R7), they show the highest values of CLD. Moreover, R6 presents again the highest CLD of the studied compounds. This was observed in all studied techniques. However, again, some differences can be noticed. In the TSSR results, the CLD of sample R4 is higher than those in R7 and R2. As discussed before, this outcome is the result of the effects of the different interactions present in this sample in the calculation of CLD. The sum of the influence of the filler–polymer and filler–filler interactions leads to a higher CLD than sample R7, where the filler–filler interactions are lower.

From the samples with covering agent, sample R8 presents the lowest CLD, due to the further reduction in the filler–filler interactions due to the addition of CA during mixing and the absence of a silica–rubber coupling. Sample R3 presents an unexpected high value; in this case, the small amount of CA added in this compound is not sufficient enough to avoid the formation of a strong filler network.

Correlation between the different techniques

The results of the evaluation of the crosslink data using equilibrium swelling, Mooney–Rivlin theory, freezing point depression temperature and TSSR experiments are shown in Fig. 10. In order to be able to compare all methods, a relative value of CLD was calculated. For the determination of this absolute CLD for each method, the crosslink density of the sample R6 of each technique was taken as the 100% value. All other values were calculated relative to this 100% value.

It can be observed that all CLD results obtained with different analytical methods present a similar trend. However, as already observed above, there are some differences between the results obtained with each technique. These differences

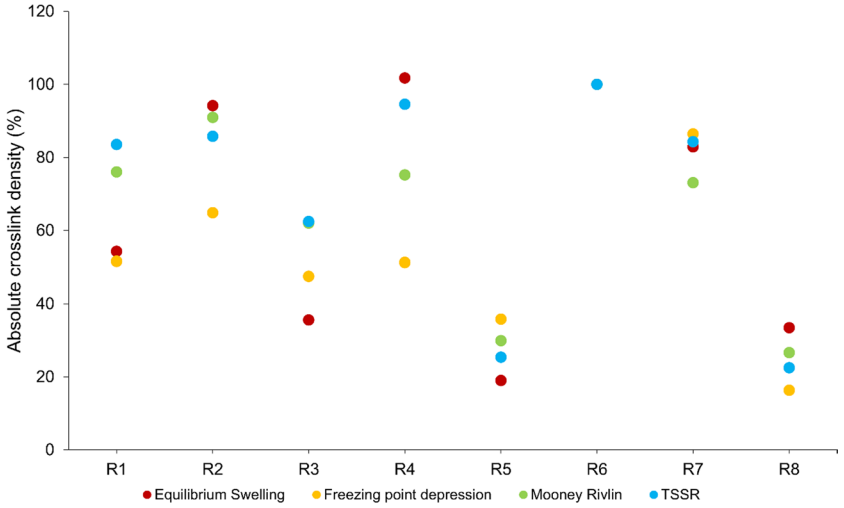

Fig. 10 Comparison between the different techniques used to measure crosslink density

are related to the dominating influence of the interactions present in each compound (Table 3). The methods are sensitive in a different way to these different interactions.

For a further analysis, the correlation strength between these different methods was calculated in form of R^2 values (Table 4). The best correlation is obtained between Mooney–Rivlin and TSSR results, with an R^2 of 0.92 (Fig. 11). However, despite the good correlation between the results of TSSR and Mooney–Rivlin, differences in the results of samples *R2* (in-situ silanized with TESPD) and R4 (pre-silanized with TESDP) can be noticed. For TSSR results, the sample in which the silica was pre-modified shows a higher CLD. The opposite occurs for the stress–strain experiments. This could indicate that results obtained by the application of the Mooney–Rivlin theory are slightly more affected by the filler effects than in the TSSR measurements. In a previous study [33], it was analyzed that an ex-situ silanization was more effective than an in-situ silanization with TESPD, showing lower filler–filler interactions. **Therefore, the higher value obtained for** *R2* in the stress–strain could be explained by the stronger filler

Table 4 Values of R2 for the linear correlation between the different techniques

Correlation	R^2
Equilibrium swelling—Mooney–Rivlin	0.73
Equilibrium swelling—Freezing point depression	0.55
Equilibrium swelling—TSSR	0.79
Mooney–Rivlin—Freezing point depression	0.71
Mooney–Rivlin—TSSR	0.92
Freezing point depression—TSSR	0.64

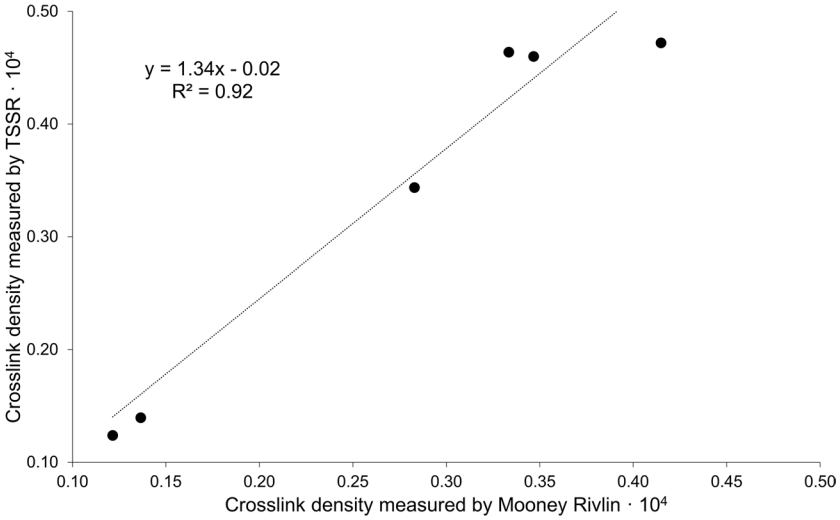

Fig. 11 Correlation between Mooney Rivlin and TSSR results

network in this sample. These indicates that in the Mooney–Rivlin approach, these interactions have a more pronounced effect.

In Table 3, it can also be observed that the other two techniques (equilibrium swelling and freezing point depression experiments) show a poor correlation between each other and with Mooney–Rivlin and TSSR. As discussed before in this study, this result can be explained by the great impact that the filler–filler interactions have on both measurements. In both techniques, the samples in which these interactions are stronger (Table 3) show a much higher CLD than expected. The poor correlation between each other also could be caused by the differences of the two methods: use of different solvents (cyclohexane and toluene) and different days of swelling of the samples (3 days for freezing point depression and 7 for equilibrium swelling).

Correlation of the different techniques with in-rubber properties

In order to the determinate, if the results of CLD calculated with each technique are in agreement with other in-rubber properties, a correlation with the modulus at 300% strain ($M_{300\%}$) and the hardness of the compounds was made. The values of R^2 obtained for each correlation are shown in Table 5. Additionally, Figs. 12 and 13 present the correlations between TSSR and Mooney–Rivlin results with the modulus at 300% strain ($M_{300\%}$) and the hardness.

On the one hand, the results of CLD obtained with TSSR and Mooney–Rivlin show the best correlation with the hardness and the $M_{300\%}$ of the studied compounds. This outcome indicates that the CLD obtained by TSSR or Mooney–Rivlin can be used as a reliable tool to predict other in-rubber properties. On the other

Table 5 Correlation of the crosslink density obtained with the different techniques with the hardness and the modulus at 300% strain of the studied compounds

Correlation with hardness	R2	Correlation with M300%	R2
Equilibrium swelling	0.69	Equilibrium swelling	0.77
Freezing point depression	0.53	Freezing point depression	0.59
TSSR	0.96	TSSR	0.87
Mooney–Rivlin	0.83	Mooney–Rivlin	0.90

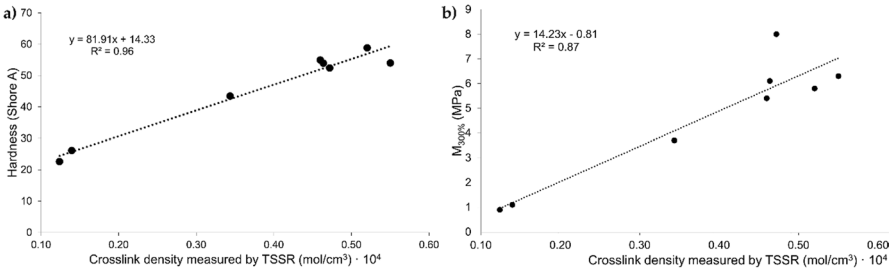

Fig. 12 Linear correlation between TSSR results with **a** hardness and **b** modulus at 300% strain of the studied compounds

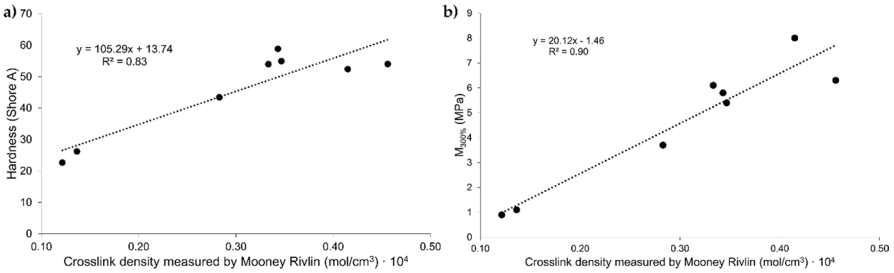

Fig. 13 Linear correlation between Mooney Rivlin results with **a** hardness and **b** modulus at 300% strain of the studied compounds

hand, as expected, the freezing point depression and equilibrium swelling experiments results present a lower correlation to the analyzed in-rubber properties.

Conclusions

In this work, four types of experimental methods to measure the crosslink density were evaluated: equilibrium swelling, stress–strain measurements based on the Mooney–Rivlin theory, freezing point depression temperature and TSSR experiments. The study of the crosslink density was performed on SBR/silica compounds prepared using in-situ and ex-situ silanization.

The analysis of this study showed that all the investigated methods are appropriate for the determination of the crosslink density of rubber compounds. It also was observed that CLD in silica-filled compounds is highly affected by different factors such as the filler–filler interactions or the type of modifying agent used. The results from all the methods present high consistency in the obtained trends for crosslink density. For all of them, higher values of this parameter were obtained for the samples containing TESPD in the formulation. It was also noticed that the compounds with mono-functional silane present the lower values of CLD. Moreover, all four techniques revealed that the sample filled with unmodified silica (R1) showed a surprisingly high crosslink density. This result could indicate that the filler network has a strong influence on the calculation of this parameter.

This study also revealed some limitations in the determination of crosslink density for filled compounds. As observed by the results obtained for sample R1 (unmodified silica), all techniques were affected by the presence of strong filler network in this compound. However, this effect was more evident in the case of equilibrium swelling experiments and freezing point depression. There are some uncertainties in the experiments and calculations of the results that are related to the presence of fillers. The restriction of the swelling behavior of the samples due to the presence of particles (non-swellable elements) leads to an overestimation of the CLD using these methods. As a consequence, the values of CLD obtained with these techniques are significantly higher for samples with a strong filler network than the ones achieved with the Mooney–Rivlin theory or the TSSR measurements.

Comparing the results of CLD between each technique, TSSR and Mooney–Rivlin show the best correlation between each other. Moreover, they also show a good correspondence with in-rubber properties of the studied compounds. For all these reasons, it could be concluded that equilibrium swelling and freezing point depression temperature are good qualitative methods that can be used in order to compare samples with the same filler loading. For a more accurate quantitative analysis and less time consuming, stress–strain experiments using the Mooney–Rivlin theory or TSSR measurements are more appropriate.

Acknowledgements The authors thank Bridgestone EMIA for the scientific and financial support as well as the permission to publish this paper.

Funding Funding provided by Bridgestone EU NV/SA.

References

1. White JR (2001) Rubber Technologist's Handbook, Rapra Tech, Rapra Technology Limited
2. Thomas S, Maria HJ (2016) Progress in rubber nanocomposites. Elsevier, Amsterdam
3. Das Gupta S, Mukhopadhyay R, Baranwal KC, Bhowmick AK (2013) Reverse engineering of rubber products. CRC Press, Boca Raton
4. De Gennes PG (1971) Reptation of a polymer chain in the presence of fixed obstacles. J Chem Phys 55:572–579. https://doi.org/10.1063/1.1675789
5. Fredrickson GH (1996) The theory of polymer dynamics. Curr Opin Solid State Mater Sci 1:812–816. https://doi.org/10.1016/S1359-0286(96)80106-9
6. De Gennes PG (1976) Dynamics of entangled polymer solutions. I. The rouse model. Macromolecules 9:587–593. https://doi.org/10.1021/ma60052a011
7. Rouse PE (1953) A theory of the linear viscoelastic properties of dilute solutions of coiling polymers. J Chem Phys 21:1272–1280. https://doi.org/10.1063/1.1699180
8. Heinrich G, Straube E, Helmis G (1988) Rubber elasticity of polymer networks: theories. Adv Polym Sci 85:33–87. https://doi.org/10.1007/bfb0024050
9. Mark FR, Erma JE, Eirich B (1953) Science and Technology of Rubber, 990–998. https://doi.org/10.1111/j.2042-7158.1953.tb14065.x
10. Strobl G (1974) The physics of polymers. Concepts Underst Struct Behav. https://doi.org/10.1016/0032-3861(74)90120-7
11. Seville B, Watson AA (1963) Structural characterization of Sulphur Network, 100–148
12. Flory PJ, Rehner J (1943) Statistical mechanics of cross-linked polymer networks II. Swelling. J Chem Phys 11:521–526. https://doi.org/10.1063/1.1723792
13. Mooney M (1940) A theory of large elastic deformation. J Appl Phys 11:582–592. https://doi.org/10.1063/1.1712836
14. Rivlin RS, Saunders DW (1951) Large elastic deformations of isotropic materials VII. Experiments on the deformation of rubber. Philos Trans R Soc Lond Ser A Math Phys Sci 243:251–288. https://doi.org/10.1098/rsta.1951.0004
15. Imanishi Y, Adachi K, Kotaka T (1988) Further investigation of the dielectric normal mode process in undiluted cis-polyisoprene with narrow distribution of molecular weight. J Chem Phys 89:7585–7592. https://doi.org/10.1063/1.455244
16. Saalwächter K, Ziegler P, Spyckerelle O, Haidar B, Vidal A, Sommer JU (2003) 1H multiple-quantum nuclear magnetic resonance investigations of molecular order distributions in poly(dimethylsiloxane) networks: evidence for a linear mixing law in bimodal systems. J Chem Phys 119:3468–3482. https://doi.org/10.1063/1.1589000
17. Bandzierz KS, Reuvekamp LAEM, Przybytniak G, Dierkes WK, Blume A, Bieliński DM (2018) Effect of electron beam irradiation on structure and properties of styrene-butadiene rubber. Radiat Phys Chem 149:14–25. https://doi.org/10.1016/j.radphyschem.2017.12.011
18. Boonstra BB, Heckman FA, Taylor GL (1968) Anomalous freezing point depression of swollen gels. J Appl Polym Sci 12:223–247. https://doi.org/10.1002/app.1968.070120201
19. Valentín JL, López-Manchado MA, Rodríguez A, Marcos-Fernández A, González L (2005) Solvent freezing point depression as a new tool to evaluate rubber compound properties. KGK Kaut Gummi Kunstst 58:503–506. https://doi.org/10.13039/501100007273
20. Barbe A, Bökamp K, Kummerlöwe C, Sollmann H, Vennemann N, Vinzelberg S (2005) Investigation of modified SEBS-based thermoplastic elastomers by temperature scanning stress relaxation measurements. Polym Eng Sci 45:1498–1507. https://doi.org/10.1002/pen.20427
21. Srinivasan N, Bökamp K, Vennemann N (2005) New test method for the characterisation of filled elastomers. KGK Kaut Gummi Kunstst 58:650–655
22. Blume A, Kiesewetter J (2019) Determination of the crosslink density of tire tread compounds by different analytical methods. KGK Kaut Gummi Kunstst 72:33–42
23. Chatterjee T, Vennemann N, Naskar K (2018) Temperature scanning stress relaxation measurements: a unique perspective for evaluation of the thermomechanical behavior of shape memory polymer blends. J Appl Polym Sci 135:45680. https://doi.org/10.1002/app.45680
24. Frenkel J (1940) A theory of elasticity, viscosity and swelling in polymeric rubber-like substances. Rubber Chem Technol 13:264–274. https://doi.org/10.5254/1.3539509
25. Flory PJ (1991) Principles of Polymer Chemistry. https://doi.org/10.1016/s0003-2670(00)80234-2

26. Heinrich G (1993) Contribution of entanglements to the mechanical properties of carbon black filled polymer networks. Macromolecules 26:1109–1119
27. Domurath J, Saphiannikova M, Heinrich G (2017) The concept of hydrodynamic amplification in filled elastomers. KGK Kaut Gummi Kunstst 70:40–43
28. Grobler JHA, McGill WJ (1993) Anomalous freezing point depression of solvents in a swollen homogeneous rubber network. J Polym Sci Part B Polym Phys 31:575–577. https://doi.org/10.1002/polb.1993.090310508
29. Honiball D, Huson MG, McGill WJ (1988) A nucleation theory for the anomalous freezing point depression of solvents in swollen rubber gels. J Polym Sci Part B Polym Phys 26:2413–2431. https://doi.org/10.1002/polb.1988.090261203
30. Jackson CL, McKenna GB (1991) On the anomalous freezing and melting of solvent crystals in swollen gels of natural rubber. Rubber Chem Technol 64:760–768. https://doi.org/10.5254/1.3538588
31. Kuhn W, Peterli E, Majer H (1955) Freezing point depression of gels produced by high polymer network. J Polym Sci 16:539–548. https://doi.org/10.1002/pol.1955.120168238
32. Kuhn W (1960) Relation between the anomalous freezing point depression and the mechanical-elastic behavior of gels. Rubber Chem Technol 33:245–253. https://doi.org/10.5254/1.3542140
33. Bernal-Ortega P, Anyszka R, Morishita Y, Di Ronza R, Blume A (2021) Comparison between SBR compounds filled with in-situ and ex-situ silanized silica. Polym (Basel) 13:1–15. https://doi.org/10.3390/polym13020281
34. Norbert V (2012) Characterization of Thermoplastic Elastomers by Means of Temperature Scanning Stress Relaxation Measurements, Thermoplast. Elastomers. https://doi.org/10.5772/35976
35. Treloar LRG (1971) Rubber elasticity. Contemp Phys 12:33–56. https://doi.org/10.1080/00107517108205104
36. Mark JE (2007) Rubber elasticity. Kobunshi 56:12–13. https://doi.org/10.1295/kobunshi.56.12
37. Chan BL, Elliott DJ, Holley M, Smith JF (1974) Influence of curing systems on the properties of natural rubber. J Polym Sci Part C Polym Symp 86:61–86. https://doi.org/10.1002/polc.5070480108
38. van Krevelen DW (2009) Properties of polymers: their correlation with chemical structure; their numerical estimation and prediction from additive group contributions, Fourth Edi, Elsevier B.V., Amsterdam, Netherlands
39. Valentín JL, Mora-Barrantes I, Carretero-González J, López-Manchado MA, Sotta P, Long DR, Saalwächter K (2010) Novel experimental approach to evaluate Filler-Elastomer interactions. Macromolecules 43:334–346. https://doi.org/10.1021/ma901999j
40. López-Manchado MA, Valentín JL, Herrero B, Arroyo M (2004) Novel approach of evaluating polymer nanocomposite structure by measurements of the freezing-point depression. Macromol Rapid Commun 25:1309–1313. https://doi.org/10.1002/marc.200400148
41. Bernal-Ortega P, Bernal MM, González-Jiménez A, Posadas P, Navarro R, Valentín JL (2020) New insight into structure-property relationships of natural rubber and styrene-butadiene rubber nanocomposites filled with MWCNT. Polym (Guildf) 201:122604. https://doi.org/10.1016/j.polymer.2020.122604
42. Bernal-Ortega P, Bernal MM, González-Jiménez A, Posadas P, Navarro R, Valentín JL (2020) Erratum to "New insight into structure-property relationships of natural rubber and styrene-butadiene rubber nanocomposites filled with MWCNT" [Polymer 201 (2020) 122604] (Polymer (2020) 201, (S0032386120304353), (https://doi.org/10.1016/j.polymer.2020.122604)), Polymer (Guildf). 203:122604. https://doi.org/10.1016/j.polymer.2020.122720
43. Valentín JL, Carretero-González J, Mora-Barrantes I, Chassé W, Saalwächter K (2008) Uncertainties in the determination of cross-link density by equilibrium swelling experiments in natural rubber. Macromolecules 41:4717–4729. https://doi.org/10.1021/ma8005087